Rapid Direct Laser Writing of Microoptical Components on A Meltable Biocompatible Gel

Mihajlo D Radmilović
Institute of Physics Belgrade: Univerzitet u Beogradu Institut za Fiziku
Branka D. Murić
Institute of Physics Belgrade: Univerzitet u Beogradu Institut za Fiziku
Dušan Gujić
Institute of Physics Belgrade: Univerzitet u Beogradu Institut za Fiziku
Boban Zarkov
Directorate for Measures and Precious Metals
Marija Z. Nenadić
Institute for Biological Research "Sinisa Stankovic"
Dejan V Pantelic (pantelic@ipb.ac.rs)
Institute of Physics Belgrade https://orcid.org/0000-0002-2027-4696

Research Article

Keywords: Laser writing, microoptics, hydrogels, biocompatibility, security.

Posted Date: November 30th, 2021

DOI: https://doi.org/10.21203/rs.3.rs-1077113/v1

Abstract

Microoptical components are coming of age in a wide range of applications: lab-on-a-chip, imaging, detection... There are a large number of fabrication technologies capable of producing high quality individual components and their arrays. However, most of them require high-end and costly equipment, complex and time-consuming fabrication, harmful chemicals, resulting in expensive final products. Here we present a technology capable of producing high quality microoptical components, using low-end direct laser writing on a biocompatible, environmentally friendly hydrogel, without any waste substances. Gel is locally and controllably melted while surface tension forces shape the optical component, following the laser beam profile. Process is so quick that a single microlens is fabricated in less than a second, and can be used instantly without any further processing. The technology is neither subtractive nor additive, and the base material is simply displaced producing a smooth surface. We have been able to fabricate individual microlenses and their arrays (positive, negative, aspheric), gratings and diffractive components. The technology is tested by generating unique, difficult to counterfeit QR-codes. Turnaround time is fast and makes the technology suitable both for rapid prototyping and serial production.

1 Introduction

There is a growing need for complex microoptical devices (Kemme 2009) and their use for micro-optoelectromechanical (MOEMS) and lab-on-a-chip applications. However, their fabrication is usually a complex, time consuming, multistep process, requiring several high-end technologies: microlithography (Grigaliūnas et al. 2016), embossing (Moore et al. 2016), femtosecond direct laser writing (Deng et al. 2019), diamond turning (Zhou et al. 2011; Zhang et al. 2020). These are the reasons why prevailing microfabrication methods are not suitable for individualized production or rapid prototyping. Also, materials used for microfabrication are complex and usually toxic. Huge volume of fabricated devices enhances the problem of safe and environmentally friendly disposal of microfabricated devices.

Among other materials, gels have attracted attention as a candidate material for MOEMS. There is a wide variety of gels with characteristic solid-liquid transition induced by coil to helix transformation (Taylor et al. 2017). The transition can be induced by temperature, chemicals or electric field. Not so many of them have good optical properties and only a few of appropriate ones are ease to fabricate, nontoxic and environmentally friendly. Optical gels (Duarte-Quiroga and Calixto. 2000; Li et al. 2019) have been used to manufacture dynamical and responsive microlenses. However, their response is slow and chemistry complex (Guan and Zhang 2011).

Microlenses have found application niches for illumination (Lee et al. 2013), imaging (Zhang et al. 2020) and, in particular, security (Walger et al. 2020). Applied technologies are advanced and complex favoring mass production and precluding individualization of security features (Jiang et al. 2019).

Here we present a technology based on nontoxic, environmentally friendly gels which are locally melted by direct laser writing. Our aim was to develop a material that is optically transparent, easily and instantly

meltable by localized irradiation, durable and made from ordinary “kitchen” chemicals (by E number classification of food additives). We describe material properties, its biocompatibility, analyze the process of local laser-induced melting, demonstrate its capabilities for security purposes and envision their further use for microfluidic and lab-on-a-chip applications.

2 Materials And Methods

2.1 Preparation of photo-meltable gel

Previously we have used gelatin plasticized with tot’hema (an oral solution for anemia treatment) and sensitized with eosin Y (a red fluorescent dye with absorption maximum at 530 nm) to produce microoptical components (Murić et al. 2007; Murić et al. 2008). We were able to manufacture negative (concave) microlenses, but the problem was gradual darkening of the material. That is why we replaced a commercial tot’hema with a water solution composed of several ingredients acting as a plasticizers, humectants, and preservatives. This solution (designated PS for brevity) consists of: 0.2 ml of glycerol, 0.3 g of sucrose, 8 mg of glucose, 2 µl of polysorbate 80, 6 mg of citric acid, and 2 mg of sodium benzoate (everything is expressed per 1 ml of solution). The addition of PS improves mechanical and optical properties of the gelatin layer (elasticity, durability and stability, optical transparency…).

After swelling of gelatin in deionized water for one hour, and heating at 50^{o}C in water bath (Vela™, Cole Parmer), 5% aqueous gelatin solution was prepared. Following, 0.01 g of sodium chloride and 0.16 ml of PS were further added (with stirring) to prevent gelatin layer crystallization and breaking. The preparation of photo-meltable gel (PMG) is concluded by adding 20 µl of eosin (2% aq. sol.). Quantity of all added components is expressed per 1 ml of gelatin solution. Finally, the PMG solution was centrifuged (Cole Parmer 17250-10 at 3400 rpm/min) in order to remove all particulates and impurities.

A PMG layer was prepared by the gravity settling method, i.e. by pouring a constant volume of prepared solution onto precisely leveled and well cleaned microscope glass slide bounded by a Plexiglas frame. After gelation, layers were left in the dark overnight, under ordinary environmental conditions (T=25^{o}C, RH=50-60%). During that time, certain amount of water evaporated from the layer, as verified gravimetrically. After reaching equilibrium value, the water content remains constant. The thickness of the dried layer depends on the amount of poured solution, and can be chosen anywhere between several tens of microns up to several millimeters or even centimeters. In our experiments, layer thickness was kept at 100 µm.

2.2 Direct laser writing system

We used a home-made laser writing device (Zarkov et al. 2012) operating at 488 nm laser (Toptica iBEAM SMART with maximum power of 100 mW). The laser beam is focused by the long working distance objective (Mitutoyo, 20x0.42 NA). Compact, color scientific CMOS camera (Thorlabs CS505CU 5 Megapixel), was used to position the PMG layer at the desired position with respect to the focal point. A coordinate stage (Ludl BioPoint2, resolution 50 nm, repeatability 2 µm) with G-code enabled Arduino

microcontroller was used to move the layer with respect to the laser beam. G-code (a standard programming language for CNC machines (Walger et al. 2020) was used to control movement with adjustable speed. Appropriate software was written to coordinate and synchronize the layer movement with laser switching and intensity adjustment.

2.3 Nonlinear microscopy of microoptical surfaces

To characterize the structure of microoptical components, we used a home-made nonlinear microscope (NLM) (Rabasović et al. 2015) equipped with a femtosecond TI:Sapphire laser (Coherent, Mira, 900F). The pulse duration is 160 fs with a 76 MHz repetition rate and average power of 100 mW. A galvo-mirror scanning system was used for raster-scanning of the samples in a commercial microscope (Leica). In order to fill the entrance pupil of microscopic objective (Carl Zeiss, 20x0.8 air) the laser beam was expanded. A tube lens produces an image on the photomultiplier tube (PMT). Images were acquired and processed using dedicated software. The spatial resolution of scanning system was 0.6 – 0.9 μm in lateral direction, while the axial resolution was 2.1 μm. Device turned out to be particularly suitable for analysis of generated microstructures due to its ability to “see” internal structure of the material.

2.4 Thermal analysis of micro-component manufacturing process

Throughout the research we used a thermal imaging to monitor thermal effects of the laser radiation during micro-component manufacturing. A commercial thermal camera (FLIR A65) with 640x512 pixels spatial resolution, 30 fps speed, thermal resolution/NETD 50 mK and 7.5-13μm spectral range was utilized to record temperature and its spatial distribution. We used an additional IR (ZnS) lens, placed in front of germanium camera lens, to further magnify the thermal image of a laser-melted zone.

2.5 *In vitro* biocompatibility testing

Cytotoxicity of tested PMG was determined on spontaneously immortalized keratinocyte cell line (HaCaT) using crystal violet assay as described previously (Stojković et al. 2020) with some modifications. HaCaT cells were grown in high-glucose Dulbecco's Modified Eagle Medium (DMEM) supplemented with 10% fetal bovine serum (FBS), 2 mM L-glutamine and 1% penicillin and streptomycin (Invitrogen), at 37°C in a 5% CO_2 incubator. Forty-eight hours before treatment, cells were seeded in a 96-well microtiter adhesive plate at a seeding density of 4 x 10^3 cells per well. PMG was dissolved in 0.01 mM PBS to a final concentration of 8 mg mL^{-1}. After 48 h, the medium was removed and the cells were treated for next 24 h with various concentrations of the dissolved gel in triplicate wells. Subsequently, the medium was removed; the cells were washed twice with PBS and stained with 0.4% crystal violet staining solution for 20 min at room temperature. Afterwards, crystal violet staining solution was removed; the cells were washed in a stream of tap water and left to air dry at room temperature. The absorbance of dye dissolved in methanol was measured in a plate reader at 570 nm (OD_{570}). The results were expressed as relative growth inhibition (GI_{50}) rate (%) indicating 50% inhibition of proliferation of HaCaT cells when compared with untreated control. Experiments were performed in triplicate for each concentration of the samples

and three independent experiments were performed. The criterion used to categorize the antiproliferative activity of PMG to HaCaT cell line was as follows: $IC_{50} \leq 20$ µg mL^{-1}= highly cytotoxic, IC_{50} ranged between 31 and 200 µg mL^{-1}= moderately cytotoxic, IC_{50} ranged between 201 and 400 µg mL^{-1}= weakly cytotoxic, and IC_{50}> 401 µg mL^{-1} = no cytotoxicity (Stojković et al. 2020).

3 Results

3.1 Material characterisation

PMG is designed to be sensitive to the wavelength of the laser used in this research (488 nm) in order to enable photo-induced melting. The focused laser beam locally heated the PMG above its melting temperature and surface tension produced a concave dip. The process was observed using a thermal camera. Temperature field is localized to the vicinity of a laser beam. Within 1/5 s, the temperature reaches maximum and decays in spite of material being still irradiated. This is due to the bleaching of eosin and the corresponding reduced absorption. This is associated with the layer turning transparent instead of red.

Surface quality of a dip is high and it acts as a concave (negative power) microlens (Krmpot et al. 2013) whose characteristics depend on the laser power, irradiation time and the laser beam size. We used NLM to characterize the surface shape and structure of a microlens. As can be seen (Fig. 1(a)), the shape of a dip is a deep asphere which produces a high quality image in its central part.

Figure 1a 3D image of a microlens shape recorded by NLM, **b** Optical microscope image showing how the size of a microlens strongly depends on the size of the laser beam

The sensitivity threshold for a 100 µm thick PMG layer is 10^4 W/cm^2, which we achieved with only 7.5 mW of laser power. This limit depends on the layer thickness, PS and dye concentrations, focus depth. It is important to mention that layer is also sensitive below 7.5 mW, but the material is only bleached (without lens formation).

As can be seen, exposure and bleaching are intertwined. We have observed the process by measuring the decrease of PMG fluorescence during irradiation, i.e. energy absorbed by the material is dissipated through fluorescence (see Fig.2). As a consequence, after certain irradiation time, layer bleaches so much to drop the temperature below the melting point. In that case, material cannot remain liquid and “freezes” its lens-like shape.

We have developed a simplified thermal model which describes temperature *T* and its dependence on initial temperature T_0:

$$T = T_0 + \frac{A}{Kmc} + \frac{B}{C-A} \bullet exp\,(-At) - (\frac{B}{C-A} + \frac{A}{Kmc})exp\,(-Ct)$$

1

The model includes constants *A*, *B*, *C* and *D* which depend on PMG layer properties: conductivity, specific heat and thickness. Additional constant *K* describes bleaching speed, while *m* is mass of the irradiated gel and *c* is specific heat (see Appendix).

Calculations have shown close correspondence with experimentally recorded temperature variation (Fig. 3b) and correctly describe initial temperature rise with subsequent exponential temperature drop (Eq. 1).

It is important to note that if the laser radiation is too intense it might occur that material can be bleached to fast so that melting temperature cannot be reached. We have experimentally observed this particular behaviour, which leaves material bleached without microlens being produced.

That is why we were forced to closely control the exposure in order to preclude this kind of memory effect. The effect is important if optical micro-components are too close, because the first one bleaches a certain space in its vicinity. If we try to write the next micro-component, exposure must be increased to compensate for a significant drop of absorption due to bleaching.

However, in the following we describe how more complex surface shapes can be manufactured by carefully controlling the laser focal position, beam pattern and exposure. We have manufactured good quality positive microlenses by making an arrangement six polygonally positioned spots. The material left in the center of a polygon acqures spherical surface which acts as a positive (convex) microlens. This can be seen in a NLM image of a material (Fig. 4).

We were able to efficiently manufacture arrays of microlenses (Fig. 5a) with rather good imaging properties (Fig. 5b).

Figure 5a Reflection image of an array of 3 x 3 positive power microlenses produced by irradiating PMG layer at the vertices of an octagon, **b** Transmission images produced by the array, **c** A resolution chart as seen through the microlens.

The best results were obtained with the octagonal arrangement of dots. Their radius of curvature and the corresponding focal length can be controlled by the diameter of a polygon (Fig. 6). We have measured the spatial resolution of the PMG layer by writing a series of gratings and found that we can manufacture up to 120 lp/mm.

3.2 Positive and negative microlenses for security

Microlenses have significant security applications for document protection (Walger et al. 2019; Seidler et al. 2014; Walger et al. 2020). In a standard implementation, their effectiveness is based on Moiré effect between a microlens array and a, suitably designed, micro-pattern or another microlens array. Superposition of two overlaid arrays produces dynamic effects similar to holograms – i.e. the resulting image varies with respect to observation direction.

Difficulty of counterfeiting such pair of arrays stems from tight tolerances of microlens parameters and necessity of their strict alignment. While this seems to be an attractive security feature it is technologically complex to achieve in practice. That is why the corresponding technologies are economically viable only through mass production (usually by printing or embossing). Production of individualized, unique, hard-to-copy security elements is thus difficult and impractical.

Here we show that technology presented here offers another way to produce unique security elements quickly and easily (on the fly) by changing microlens parameters (position, sag, diameter, focal length, mutual position). We demonstrate the principle by producing a microlens-based QR-code (see Fig. 6).

Each dot of a standard 21 x 21 QR-code is a negative microlens, except for one or several selected, which are a positive. Security features are focal lengths of individual microlenses (either positive or negative) of a QR-code.

Figure 7A microlens-based QR-code in a two focal positions **a** and **b**, Butterfly wing scale **c**, image of butterfly wing scale formed on QR-code lenses **d**, Multiple images of butterfly wing scale from Fig. **c** produced by QR code microlenses

Focal length of each microlens is revealed by placing a closely positioned micro-sized object while detecting the size of its image. Here we used a butterfly wing scale as such object, positioned on the other side of a microlens substrate. Due to the wide view field of negative microlenses, image of an object is seen across several microlenses in shifted positions – yet another, difficult to copy, feature.

3.3 *In vitro* cytotoxicity of hydrogel samples towards HaCaT cells

To evaluate the cytotoxic effect of the PMG dissolved in *0.01 mM PBS* on HaCaT cells, the crystal violet assay was performed. Relative growth rate of HaCaT cells in the presence of different concentrations of tested *sample compared to* untreated *control is presented in Figure 8.* Tested sample was evaluated as non-toxic to the HaCaT cell line with respective IC_{50} values of 400 mg/mL, a concentration which is considered as the limit of toxicity (Stojković et al. 2020).

Figure 8 Relative growth rate of HaCaT cells in the presence of different concentrations of PMG

4. Discussion

Microlens fabrication enables efficient control of each individual microlens by controlling a number of process parameters: laser beam size, shape, power, angle, speed and exposure, as well as physical/chemical properties of the PMG layer. There are certain limitations, drawbacks and possibilities which will be discussed in this section

Manufacturing speed of microlenses is limited by the laser energy density (determined by the laser power and focal point size), absorbance, viscosity and surface tension of melted gel. This is a complex process difficult to model in a simple way. However, we were able to find appropriate conditions experimentally. Laser powers above 7.5 mW and exposure times longer than 100 ms gave us complete control of the process and production of predictable lens size and profile.

The material is soft and elastic due to the presence of plasticizer. Its stress-strain behavior depends on the PS concentration, as shown earlier in the case of commercial tot'hema, when the corresponding Young's moduli were between 1 and 10 MPa (Murić et al. 2013). Also, for high-concentration (30%) of tot'hema, more than 200% elongation was achieved. In the case of PMG the above properties are retained. Elasticity and stretchability can be utilized to manufacture tunable optical components.

On the other hand, softness makes material sensitive to mechanical scratching and damaging. That is why it must be protected by an additional mechanically resistant layer. Alternatively, material can be hardened by simply placing in water to let plasticizer diffuse out.

We observed the layer's surface under the polarizing microscope and noticed that there were no internal, residual stresses (material is homogeneous).

The material remains photosensitive for a long time even if exposed to normal laboratory conditions. Its shelf life is mainly determined by slow evaporation of water and photo-bleaching of sensitizer. If the atmosphere is too dry, concentration of water diminishes and constituent chemicals start crystallizing and the layer attains milky appearance. In that sense, it is preferable to keep material in a humid and light-tight container. From the practical experience, material processing can be performed under normal lighting without special precautions or dimmed light. However, we have a few years old gelatine layers, stored under normal laboratory conditions, which are still photosensitive and we were able to produce good quality microlenses. They are very stable, too, and the image quality remains constant during many months and even years under normal conditions. Of course, material has to be protected from scratches and dust as in the case of all the other optical surfaces.

The material presented here is not unique. Instead of eosin, we have tried gelatin sensitization with several natural fluorophores: anthocyanin, betanin and several other food dyes with excellent results. Additionally we have tried other gels based on chitosan and pectin with very promising results. That is why we can claim that many other gels, humectants and sensitizers can further enhance microlens production speed and surface quality.

Depending on how material is prepared, buckling induced by evaporation of solvent produces unpredictable surface pattern. Even then, re-melting of material by the laser beam flattens the surface and produces good optical component. As a result a combination of random buckling surface structure and regular optical components produce uniquely and nonreproducibly complex security features.

Yet another possibility stems from photo damage of the material, which occurs above certain power density threshold. In that case, material carbonizes, producing strongly localized damage zone in a center of the laser spot. Interestingly, this does not preclude microlens imaging, but adds a new feature to a security component.

Here we emphasize that the technology described here is neither additive nor subtractive because no material is added or removed. It is important to note that all the substances used are not volatile and the melting temperature of the material is below 50^{o}C, so that water evaporation is negligible. However, do to the melting, surface tension compresses and densifies the material. This is witnessed by the increased intensity of fluorescence at the circumference of the cavity. That is why the volume of the laser-induced dip is larger than the volume on the edge (Murić et al. 2009).

The material is complex mixture of nontoxic chemical aiming to fulfill several requirements: preventing crystallization, retention of constant amount of water, reducing the melting point of the gel, to enable efficient flow during laser melting, retaining plastic and elastic properties of the material, increasing the laser energy absorption. Proper composition was found experimentally and found to be stable before and after microlens fabrication.

Material has certain drawbacks too. It is soft, and can be easily damaged if unprotected. On the other hand, this property can be used to detect tampering and produce tamper sensitive tags. Material surface is sticky and dust particles easily adhere to its surface. Therefore, cleanliness is important factor in practical usage of the material.

We used gelatin as a base material, but the working principle is universal and can be applied to any material which can be locally melted, without damage on a sufficiently low temperature (preferably below 100 ^{o}C). In that respect we tested chitosan, too with quite good results which will be presented in the future publications.

Applications are not limited to microlenses and arbitrary structures can be manufactured such as microchannels, diffraction gratings, holograms (see Fig. 9).

Figure 9A range of microoptical structures which can be fabricated on the PMG layer – retinal vessel model (center), QR-code (top left), negative microlens array (top right), positive microlens (bottom right) array, grating (bottom left).

5 Conclusions

We have presented a new, gel-based, material suitable for fast and efficient generation of a wide range of microoptical and micromechanical components.

There are several advantages of the proposed method:

- Cheap lasers can be used as long as they have a circular laser beam profile and 2% power stability within the millisecond time interval.

- Chemicals used to produce the PMG are non-poisonous at the stated concentrations, as verified by biocompatibility tests

- Fabrication time is fast enough to enable rapid prototyping of on-demand components

- A variety of optical and micromechanical components can be fabricated within a single manufacturing operation

- Components require no further processing and can be used immediately following fabrication.

Declarations

Author Contributions

B. M. synthesized a photo-meltable material. D.G., B.Z. and D.P. constructed a laser writing device used through this research. D.P. D.G. and M. R. wrote control software. B.M. D.P. and M. R. tested material properties. M.Z.N. tested *in vitro* biocompatibility and microbial susceptibility toward synthesized gel material. D. P. Developed a thermal model of material bleaching. D.P. B.M. and M.R. jointly wrote the manuscript.

Conflicts of interest

There are no conflicts to declare.

Acknowledgements

The authors acknowledge funding provided by the Institute of Physics Belgrade, through the grant by the Ministry of Education, Science and Technological Development of the Republic of Serbia.

This research was partially funded by the NATO Science for Peace and Security programme, project SPS G5618, Biological and bioinspired structures for multispectral surveillance.

References

1. Deng, C., Kim, H., Ki, H.: Fabrication of a compound infrared microlens array with ultrashort focal length using femtosecond laser-assisted wet etching and dual-beam pulsed laser deposition. Opt.

Express. **27**, 28679–28691 (2019)

2. Duarte-Quiroga, R.A., Calixto, S.: Dynamical optical microelements on dye-sensitized gels. Appl. Opt. **39**, 3948–3954 (2000)
3. Grigaliūnas, V., Lazauskas, A., Jucius, D., Viržonis, D., Abakevičienė, B., Smetona, S., Tamulevičius, S.: Microlens fabrication by 3D electron beam lithography combined with thermal reflow technique. Microelectron. Eng. **164**, 23–29 (2016)
4. Guan, Y., Zhang, Y.: PNIPAM microgels for biomedical applications: From dispersed particles to 3D assemblies. Soft. Matter. **7**, 6375–6384 (2011)
5. ISO 6983-1:2009(en) Automation systems and integration — Numerical control of machines — Program format and definitions of address words — Part 1: Data format for positioning, line motion and contouring control systems
6. Jiang, H., Kaminska, B., Porras, H., Raymond, M., Kapus, T.: Microlens arrays above interlaced plasmonic pixels for optical security devices with high-resolution multicolor motion effects. Adv. Opt. Mater. **7**, 1–10 (2019)
7. Kemme, S.A.: Microoptics and Nanooptics Fabrication. CRC Press (2009)
8. Krmpot, A.J., Tserevelakis, G.J., Murić, B.D., Filippidis, G., Pantelić, D.V.: 3D imaging and characterization of microlenses and microlens arrays using nonlinear microscopy. J. Phys. D: Appl. Phys. **46**, 195101 (2013)
9. Lee, X-H., Moreno, I., Sun, C-C.: High-performance LED street lighting using microlens arrays. Opt. Express. **21**, 10612–10621(2013)
10. Li, Y., Guo, M., Li, Y.: Recent advances in plasticized PVC gels for soft actuators and devices: A review. J. Mater. Chem. C. **7**, 2991–3009 (2019)
11. Moore, S., Gomez, J., Lek, D., You, B.H., Kim, N., Song, I.H.: Experimental study of polymer microlens fabrication using partial-filling hot embossing technique. Microelectron. Eng. **162**, 57–62 (2016)
12. Murić, B., Pantelić, D., Vasiljević, D., Panić, B.: Microlens fabrication on tot'hema sensitized gelatin. Opt. Mater. **30**, 1217–1220 (2008)
13. Murić, B., Pantelić, D., Vasiljević, D., Panić, B., Jelenković, B.: Thermal analysis of microlens formation on a sensitized gelatin layer. Appl. Opt. **48**, 3854–3859 (2009)
14. Murić, B., Pantelić, D., Vasiljević, D., Zarkov, B., Jelenković, B., Pantović, S., Rosić, M.: Sensitized gelatin as a versatile biomaterial with tailored mechanical and optical properties. Phys. Scr. **T157**, 014018 (2013)
15. Murić, B.D, Pantelić, D.V., Vasiljević, D.M, Panić, B.M.: Properties of microlenses produced on a layer of tot'hema and eosin sensitized gelatin. Appl. Opt. **46**, 8527–8532 (2007)
16. Rabasović, M.D., Pantelić, D.V., Jelenković, B.M., Ćurčić, S.B., Rabasović, M.S., Vrbica, M.D., Lazović, V.M., Ćurčić, B.P.M., Krmpot, A.J.: Nonlinear microscopy of chitin and chitinous structures: a case study of two cave-dwelling insects. J. Biomed. Opt. **20**, 16010 (2015)

17. Seidler, R., Heim, M., Wiedner, B., Rahm, M.: Method for manufacturing security paper and microlens thread. US 2014/0238628 A1 (2014)
18. Stojković, D., Drakulić, D., Gašić, U., Zengin, G., Stevanović, M., Rajčević, N., Soković, M.: Ononis spinosa L. an edible and medicinal plant: UHPLC-LTQ-Orbitrap/MS chemical profiling and biological activities of the herbal extract. Food & Function. **11**, 7138–7151 (2020)
19. Taylor, M., Tomlins, P., Sahota, T.: Thermoresponsive gels. Gels, **3**, 1–31 (2017)
20. Walger, T., Besson, T., Flauraud, V., Hersch, R.D., Brugger, J.: 1D moiré shapes by superposed layers of micro-lenses. Opt. Express. **27**, 37419–37434 (2019)
21. Walger, T., Besson, T., Flauraud, V., Hersch, R.D, Brugger, J.: Level-line moirés by superposition of cylindrical microlens gratings. J. Opt. Soc. Am. A. **37**, 209–218 (2020)
22. Zarkov, B., Grujić, D., Pantelić, D.: High-resolution dot-matrix hologram generation. Phys. Scr. **T149**, 014021 (2012)
23. Zhang, T., Li, P., Yu, H., Wang, F., Wang, X., Yang, T., Yang, W., Li, W.J., Wang, Y., Liu, L.: Fabrication of flexible microlens arrays for parallel super-resolution imaging. Applied Surface Science, **504**, 144375 (2020)
24. Zhou, J., Sun, T., Zong, W.: A new approach to fabricate micro lens array using fast tool servo. Int. J. Nanomanuf. **7**, 475–487 (2011)

Figures

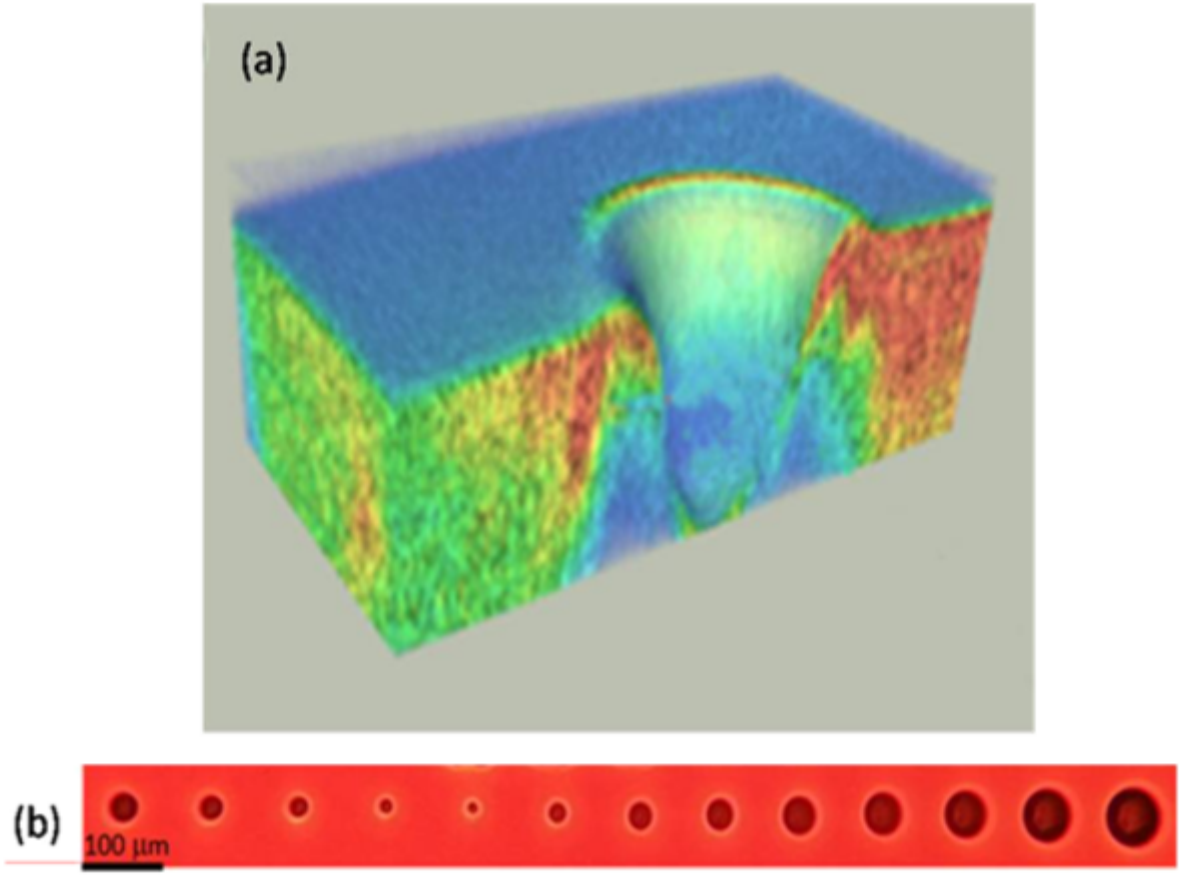

Figure 1

a 3D image of a microlens shape recorded by NLM, b Optical microscope image showing how the size of a microlens strongly depends on the size of the laser beam

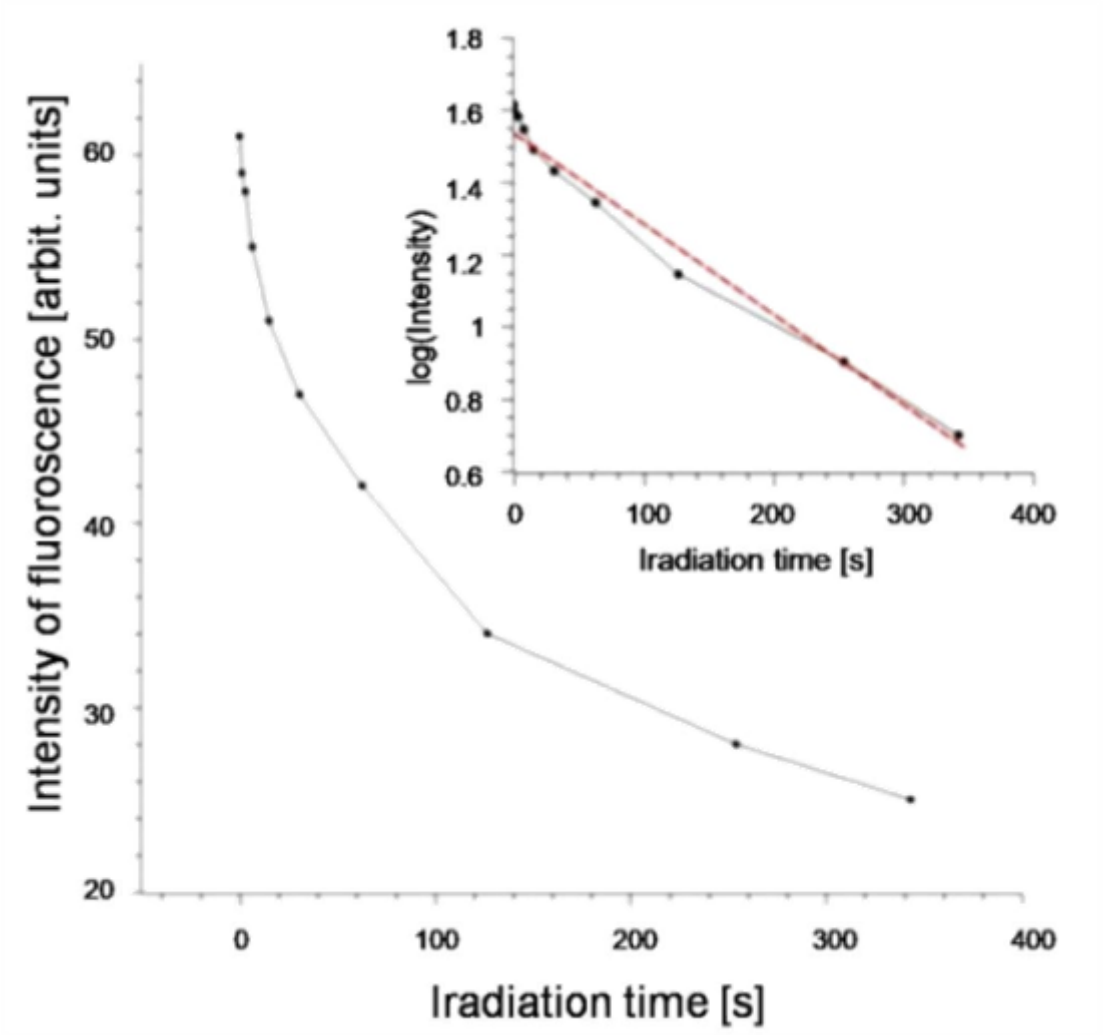

Figure 2

Bleaching of material observed as a decrease of fluorescence intensity under irradiation with 0.05 mW focused laser beam. Fluorescence decay is represented on the linear scale. The same graph, presented on a logarithmic scale, is shown in the inset.

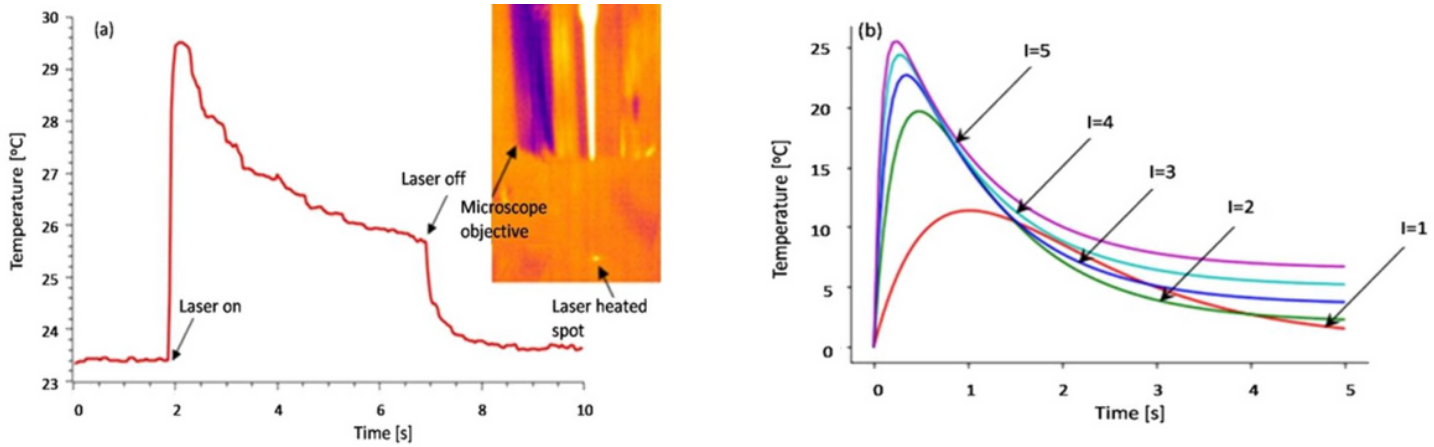

Figure 3

A temperature profile during constant-power irradiation (5s, 15 mW laser power) of PMG layer. Temperature rises with 1/5s and decreases due to bleaching of eosin. After turning the laser off, temperature quickly drops to that of the environment

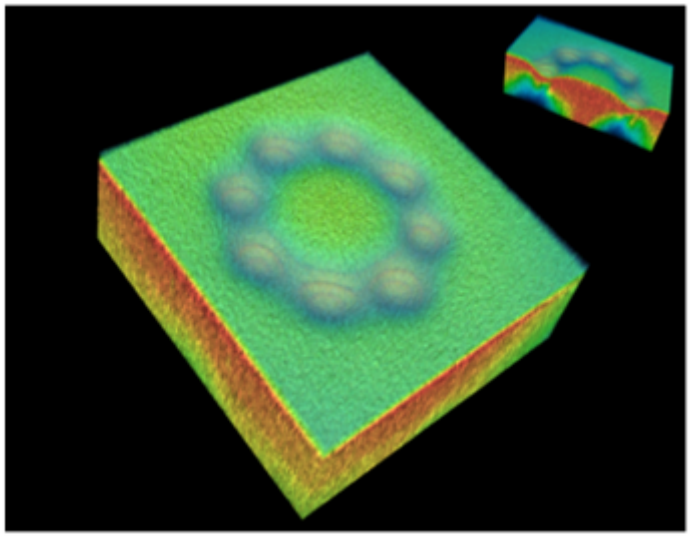

Figure 4

A NLM image of a positive microlens produced by irradiating the PMG layer at the vertices of an octagon. 3D view together with its orthogonal cross section (inset) is shown.

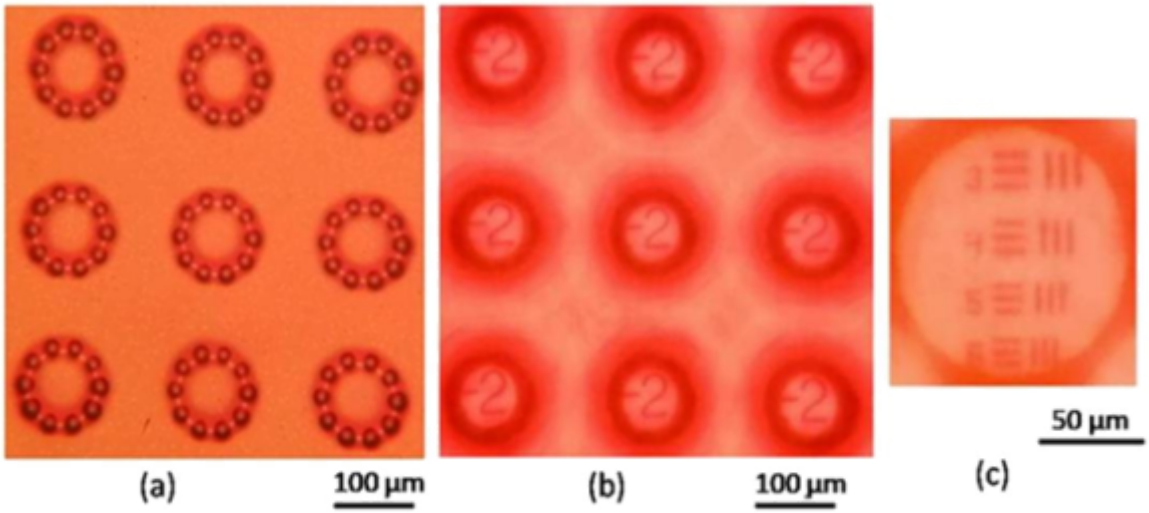

Figure 5

a Reflection image of an array of 3 x 3 positive power microlenses produced by irradiating PMG layer at the vertices of an octagon, b Transmission images produced by the array, c A resolution chart as seen through the microlens.

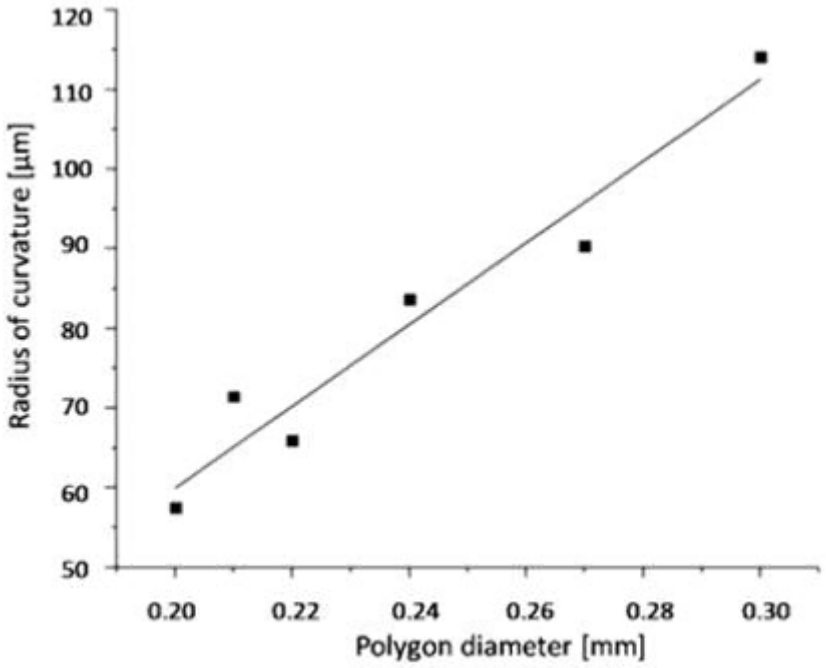

Figure 6

A linear relation between the microlens radius of curvature and the diameter of a polygonal arrangement of dots.

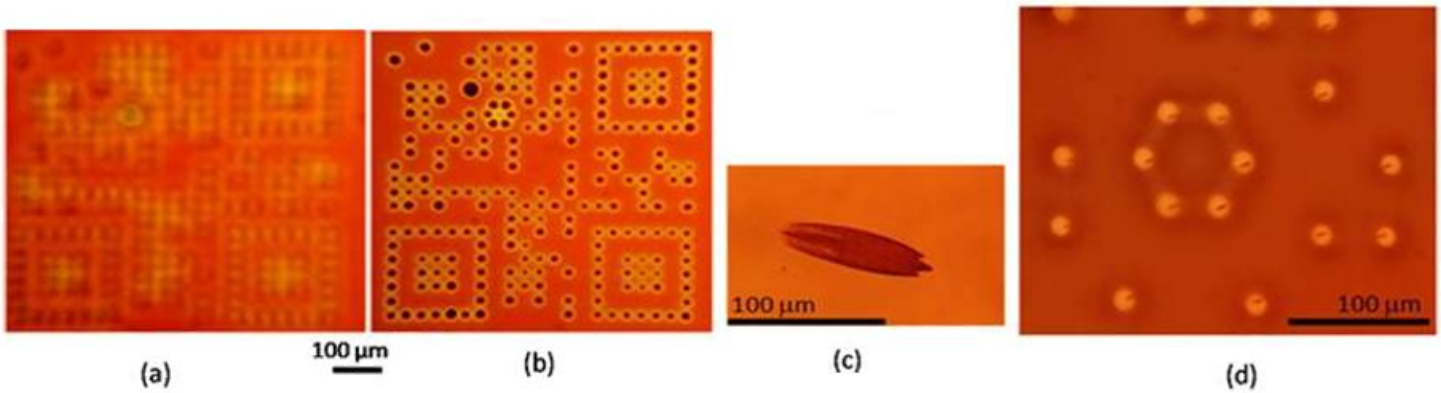

Figure 7

A microlens-based QR-code in a two focal positions a and b, Butterfly wing scale c, image of butterfly wing scale formed on QR-code lenses d, Multiple images of butterfly wing scale from Fig. c produced by QR code microlenses

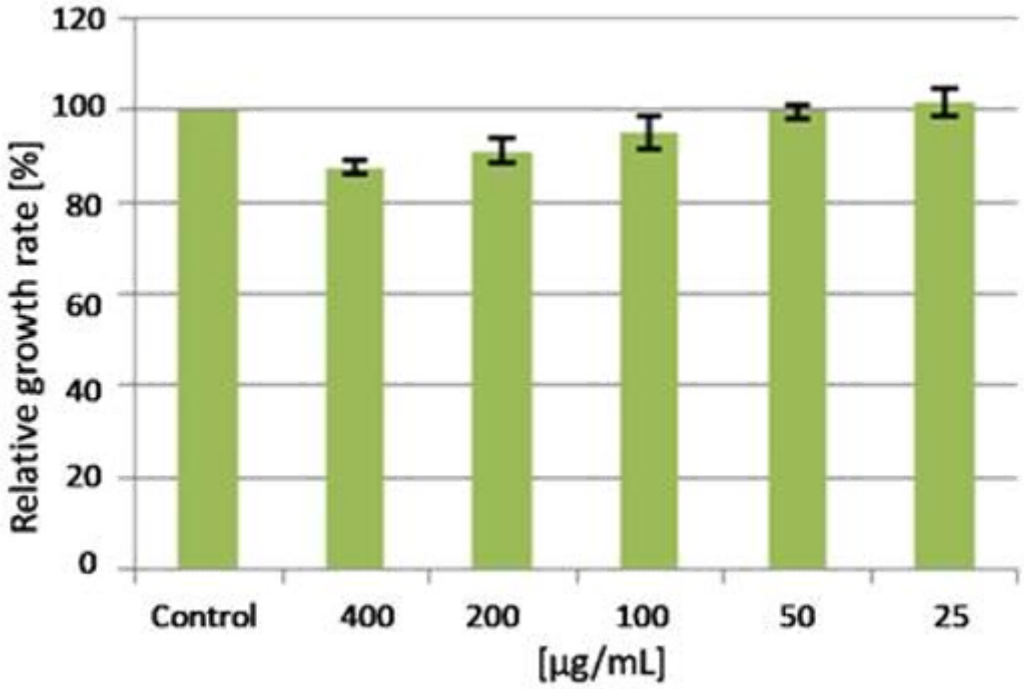

Figure 8

Relative growth rate of HaCaT cells in the presence of different concentrations of PMG

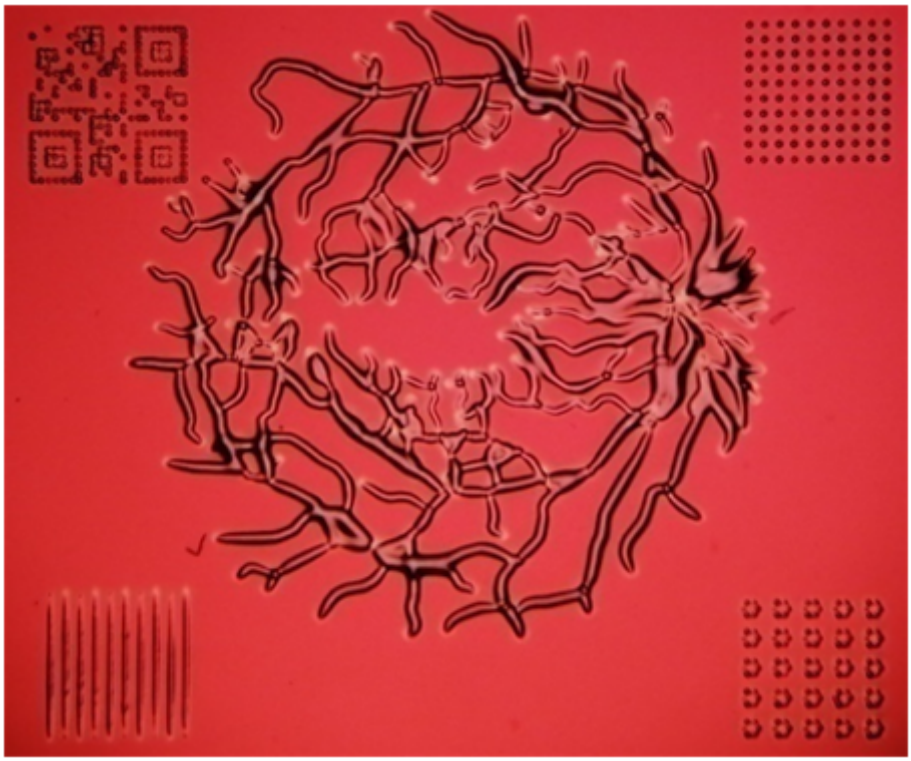

Figure 9

A range of microoptical structures which can be fabricated on the PMG layer – retinal vessel model (center), QR-code (top left), negative microlens array (top right), positive microlens (bottom right) array,

grating (bottom left).

Supplementary Files

This is a list of supplementary files associated with this preprint. Click to download.

- Photonica2021RadmilovicetalAppendix.docx